

Simulation of Incompressible Flows in Two-Sided Lid-Driven Square Cavities. Part II - LBM

D. Arumuga Perumal^{1c} and Anoop K. Dass¹

¹*Department of Mechanical Engineering,
Indian Institute of Technology Guwahati,
Guwahati-781039, INDIA*

Received: 15/10/2009 – Revised 15/01/2010 – Accepted 04/03/2010

Abstract

The present paper computes the flow in a two-sided lid-driven square cavity by the Lattice Boltzmann Method (LBM). For some aspect ratios there exists a multiplicity of steady solutions, but the square cavity problem gives only a single steady solution for both the parallel and antiparallel motion of the walls. It is found that for parallel motion of the walls, there appears a pair of counter-rotating secondary vortices of equal size near the centre of a wall. Because of symmetry, this pair of counter-rotating vortices has similar shapes and their detailed study as to how they grow with increasing Reynolds number has not yet been made by lattice Boltzmann Method. Such a study is attempted in this paper through the LBM, as the results of the problem have the potential of being used for testing various solution methods for incompressible viscous flows. The results for the antiparallel motion of the walls are also presented in some detail. To lend credibility to the LBM results they are further compared with those obtained from a finite difference method (FDM).

Keywords: *two-sided lid-driven square cavity; lattice Boltzmann method; D2Q9 model; bounce-back boundary condition; finite difference method.*

1. Introduction

Simulation of incompressible flows in two-sided lid-driven square cavity flow by FDM is discussed in some detail in the first part of our paper [1]. The present work focuses on the computation and validation of two-sided lid-driven square cavity flows by the Lattice Boltzmann Method. The LBM is a relatively novel technique that has become an alternative to the traditional numerical methods for computing fluid flow problems. The method is discussed in sufficient details in the books by Wolf-Gladrow [2] and Succi [3]. Chen and Doolen [4] have written an excellent review paper on the subject. Historically, LBM originated from the method of Lattice Gas Cellular automata (LGCA), which was first introduced in 1973 by Hardy, Pomeau and de Pazzis (HPP) [5]. In 1986, Frisch, Hasslacher and Pomeau (FHP) obtained the correct Navier-Stokes equations using a hexagonal lattice. Lattice Boltzmann Equations has been used at the cradle of Lattice Gas Automata (LGA) by Frisch et al. [6] to calculate viscosity. To eliminate statistical noise in 1988

^c Corresponding Author: D. Arumuga Perumal

Email: d.perumal@iitg.ernet.in Telephone: +91 361 2582654

Fax: +91 361 2690762

© 2009-2012 All rights reserved. ISSR Journals

McNamara and Zanetti [7] did away with the Boolean operation of LGA involving the particle occupation variables by neglecting particle correlations and introducing averaged distribution functions giving rise to the LBM. Higuera and Jimenez [8] brought about an important simplification in LBM by presenting an lattice Boltzmann Equation (LBE) with a linearized collision operator that assumes that the distribution is close to the local equilibrium state. A particularly simple version of linearized collision operator based on the Bhatnagar-Gross-Krook (BGK) [9] collision model was independently introduced by several authors including Koelman [10] and Chen et al. [11]. The lattice BGK (LBGK) model [12, 13] utilizes the local equilibrium distribution function to recover the macroscopic Navier-Stokes equations.

A review of computational and experimental studies on lid-driven cavity flow can be found in Shankar & Deshpande [14]. They have studied and analyzed corner eddies, nonuniqueness, transition and turbulence in the lid-driven cavity. The two-sided lid-driven rectangular cavity problem has been investigated in some details by Kuhlmann and coworkers [15]. Many researchers [17-20] carried out simulations of one-sided lid-driven cavity flow by the lattice Boltzmann method. Yong G Lai et al. [19] compared the lattice Boltzmann method and the finite volume Navier-Stokes solver and concluded that bounce-back boundary condition has better than first order accuracy. The present work uses Lattice Boltzmann BGK model (LBGK) with single time relaxation and bounce-back boundary condition to investigate the flow driven by parallel and antiparallel motion of two facing walls in a square cavity for Reynolds number up to 2000. A nine-velocity incompressible LB model in 2D space has been used in the present work since it is known to give more accurate results compared to seven-velocity incompressible LB model.

This paper is organized in four sections. In Section 2 numerical methods including LBGK with single time relaxation scheme and two-dimensional nine-velocity lattice model is described. In Section 3 the two-sided lid-driven cavity problem is described and the results with parallel and antiparallel motion of the walls are presented and validated. Concluding remarks are made in Section 4.

2. Numerical Methods

2.1. Lattice Boltzmann Method

As has already been mentioned the Lattice Boltzmann method (LBM) represents an alternative possibility for the direct simulation of the incompressible flow. It is seen that the accuracy of the Lattice Boltzmann method is of second order both in space and time [19]. The Lattice Boltzmann equation which can be linked to the Boltzmann equation in kinetic theory is formulated as [17]

$$f_i(\mathbf{x} + \mathbf{c}_i \Delta t, t + \Delta t) - f_i(\mathbf{x}, t) = \Omega_i \quad (1)$$

where f_i is the particle distribution function, \mathbf{c}_i is the particle velocity along the i th direction and Ω_i is the collision term. The so-called LBGK model with single time relaxation, which is a commonly used lattice Boltzmann method is given by [17]

$$f_i(\mathbf{x} + \mathbf{c}_i \Delta t, t + \Delta t) - f_i(\mathbf{x}, t) = -\frac{1}{\tau} \left(f_i(\mathbf{x}, t) - f_i^{(0)}(\mathbf{x}, t) \right) \quad (2)$$

where $f_i^{(0)}(\mathbf{x}, t)$ is the equilibrium distribution function at \mathbf{x}, t and τ is the time relaxation parameter.

2.1.1. Two-Dimensional Nine-Velocity Square Lattice Model

The *D2Q9* square lattice used here has nine discrete velocities. A square lattice is used, each node of which has eight neighbours connected by eight links as shown in Figure 1. Particles residing on a node move to their nearest neighbours along these links in unit time

step. The occupation of the rest particle is designated as f_0 . The occupation of the particles moving along the x - and y -axes are designated as f_1 , f_2 , f_3 , f_4 , while the occupation of diagonally moving particles are designated as f_5 , f_6 , f_7 , f_8 . The particle velocities are defined as

$$\begin{aligned} c_i &= 0, \quad i = 0 \\ c_i &= (\cos(\pi/4(i-1)), \sin(\pi/4(i-1))), \quad i = 1, 2, 3, 4 \\ c_i &= \sqrt{2}(\cos(\pi/4(i-1)), \sin(\pi/4(i-1))), \quad i = 5, 6, 7, 8. \end{aligned} \quad (3)$$

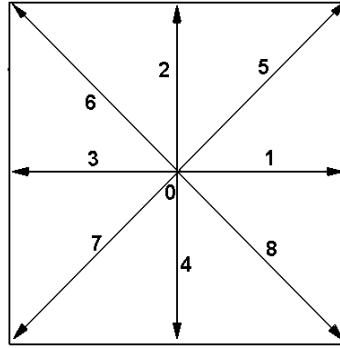


Figure 1. Two-Dimensional Nine-Velocity Square Lattice ($D2Q9$) Model.

The macroscopic quantities such as density ρ and momentum density $\rho\mathbf{u}$ are defined as velocity moments of the distribution function f_i as follows:

$$\rho = \sum_{i=0}^N f_i, \quad (4)$$

$$\rho\mathbf{u} = \sum_{i=0}^N f_i \mathbf{c}_i \quad (5)$$

The density (which is directly related to the pressure) is determined from the particle distribution function. The density and the velocities satisfy the Navier-Stokes equations in the low-Mach number limit. This can be demonstrated by using the Chapman-Enskog expansion. In the nine-speed square lattice, a suitable equilibrium distribution function that has been proposed is [17]

$$\begin{aligned} f_i^{(0)} &= \rho w_i \left[1 - \frac{3}{2} \mathbf{u}^2 \right], \quad i = 0 \\ f_i^{(0)} &= \rho w_i \left[1 + 3(\mathbf{c}_i \cdot \mathbf{u}) + 4.5 (\mathbf{c}_i \cdot \mathbf{u})^2 - 1.5 \mathbf{u}^2 \right], \quad i = 1, 2, 3, 4 \\ f_i^{(0)} &= \rho w_i \left[1 + 3(\mathbf{c}_i \cdot \mathbf{u}) + 4.5 (\mathbf{c}_i \cdot \mathbf{u})^2 - 1.5 \mathbf{u}^2 \right], \quad i = 5, 6, 7, 8 \end{aligned} \quad (6)$$

where the lattice weights are given by $w_0 = 4/9$, $w_1 = w_2 = w_3 = w_4 = 1/9$ and $w_5 = w_6 = w_7 = w_8 = 1/36$. The relaxation time is related to the viscosity by [19]

$$\tau = \frac{6\nu+1}{2} \quad (7)$$

where ν is the kinematic viscosity measured in lattice units. It is seen that $\tau = 0.5$ is the critical value for ensuring a non-negative kinematic viscosity. Numerical instability can occur for a τ close to this critical value. This situation takes place at high Reynolds numbers. In this work Reynolds numbers up to 2000 in a lattice size of 513×513 have been investigated.

2.1.2. Boundary Conditions

In LBM several boundary conditions have been proposed [17-20]. The bounce-back scheme was used in these simulations to copy the velocity no-slip condition on walls. In this scheme, the particle distribution function at the wall lattice node is assigned to be the particle distribution function of its opposite direction. The basic argument for the use of ‘on-grid bounce-back model’ is that it is both mathematically applicable and quite relevant for LBE simulations of fluid flows in simple bounded domains. For this reason, this boundary condition has been employed here on the two stationary walls. However for the moving walls, the equilibrium boundary condition is applied [17]. At the lattice nodes on the moving walls, flow-variables are re-set to their pre-assumed values at the end of every streaming-step. A lid-velocity of $U = 0.1$ has been considered in this work. Since Mach number is U/c_s , where c_s equals $1/\sqrt{3}$ a Mach number of 0.1732, well within the incompressible limit, is obtained.

2.1.3. Numerical Procedure

The velocities are assumed to be zero at the time of starting the simulations for all nodes. Initially, the equilibrium distribution function that corresponds to the flow-variables is assumed as the unknown distribution function for all node at $t = 0$. Also a uniform fluid density $\rho = 1.0$ is imposed initially. The boundary conditions for the parallel and antiparallel wall motion are shown in Figures 2 (a) and 2 (b). The solution procedure of the above LBM at each time step comprise the streaming and collision step, application of boundary conditions, calculation of particle distribution function followed by calculation of macroscopic variables. The LBE is solved in the solution domain subjected to the above initial and boundary conditions on a uniform 2D square lattice structure. It is seen that the numerical algorithm of the lattice Boltzmann method is relatively simpler compared with conventional Navier-Stokes methods that use techniques like finite difference, finite volume or finite element to discretize the equations at the macroscopic level. Another benefit of the present approach is the easiness of programming.

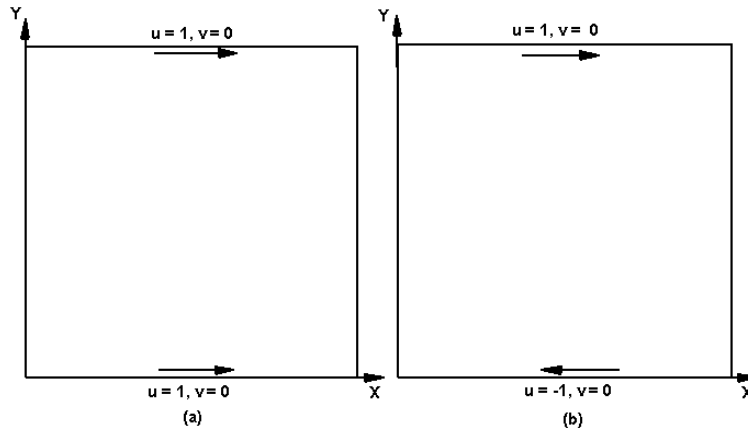


Figure 2. Two-Sided Lid-Driven Cavity for (a) parallel wall motion (b) antiparallel wall motion with LBM boundary conditions for the moving walls.

2.2. Finite Difference Results for Comparison

As the LBM method is intended to be used to compute the flow in a relatively unexplored problem, Ref [1] that uses FDM to compute the flow in the same geometry serves as an effective basis for comparison of most of the results presented in this paper. The FDM code

numerically solves the 2D Navier-Stokes equations in the stream function-vorticity form given by

$$\frac{\partial^2 \psi}{\partial x^2} + \frac{\partial^2 \psi}{\partial y^2} = -\omega \quad (8)$$

$$\frac{\partial \omega}{\partial t} + u \frac{\partial \omega}{\partial x} + v \frac{\partial \omega}{\partial y} = \frac{1}{Re} \left(\frac{\partial^2 \omega}{\partial x^2} + \frac{\partial^2 \omega}{\partial y^2} \right). \quad (9)$$

This form of the Navier-Stokes equation is known to be amenable for highly accurate numerical solution. The code, which is validated against established results, uses ADI technique and second-order accurate central differencing for space discretization. Consequently these results, which are the only ones available for comparison, are highly reliable. Thus, favourable comparison of the present LBM results with these accurate FDM results will grant legitimacy to them. This in turn would lend added credibility to the results for this relatively unexplored problem, so that the flow configuration could be used as a good test case for algorithm validation.

2.3. Validation of the LBM Code

The developed LBM code is used to compute the single lid-driven square cavity flow for $Re = 1000$ on a 129×129 lattice structure. Well-established results computed by Ghia et al. [16] exist for the same problem which is used for the present code-validation exercise. Figures 3(a) and 3(b) shows the steady-state x -component of the velocity along the vertical centreline and the y -component of the velocity along the horizontal centreline of the cavity at $Re = 1000$. Here the top lid moves from left to right and it is observed that the agreement between our LBM results and those of Ghia et al. [16] is excellent. The close agreement gives credibility to the result of our LBM code and it stands validated. The same figure also displays the FDM results [1] of the present authors, which again are in excellent agreement with these results.

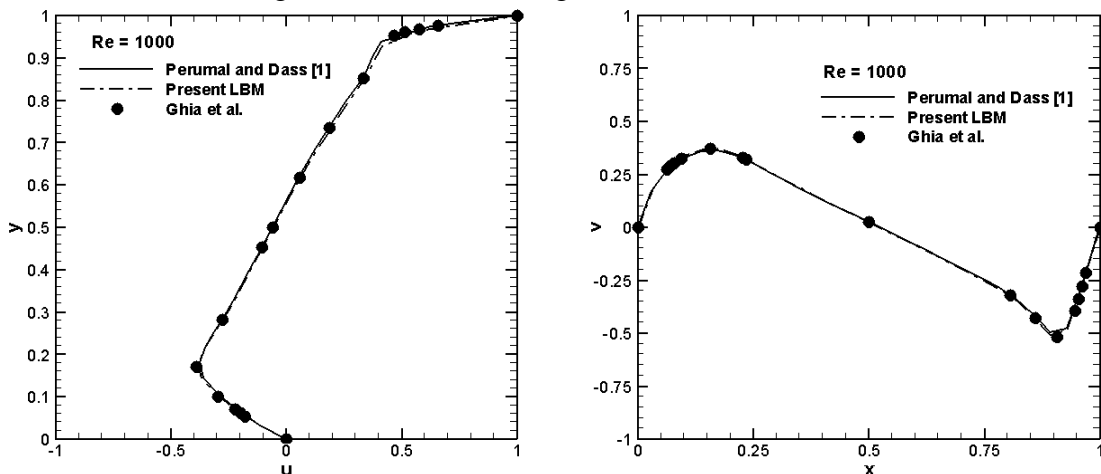


Figure 3. Code validation: (a) u -velocity along vertical centreline and (b) v -velocity along horizontal centreline for single lid-driven square-cavity ($Re = 1000$).

3. Two-Sided Lid-Driven Cavity Flow

An incompressible viscous flow in a square cavity whose top and bottom walls move in the same (parallel motion) or opposite (antiparallel motion) direction with a uniform velocity is the problem investigated in the present work. In the case of parallel wall motion, a free shear layer exists midway between the top and bottom walls apart from the wall bounded shear layers, whereas in the case of antiparallel wall motion, only wall bounded shear layers exist.

3.1. Parallel Wall Motion

In the parallel motion we consider, both the upper and lower plates move from left to right in the x direction with the same velocity. Figure 4 shows the streamline patterns for various Reynolds numbers on a 513×513 lattice structure. Expectedly, the streamlines are found to be symmetrical with respect to the horizontal centerline. Figure 4(a) shows the streamline pattern for $Re = 100$. Two counter-rotating primary vortices symmetrical to each other are seen to form with a ‘free’ shear layer in between. At this Reynolds number the primary vortex cores are seen to be somewhat away from the centres of the top and the bottom halves of the cavity towards the righthand top and righthand bottom corners respectively. Figure 4(b) shows the streamline pattern for $Re = 400$. At this Reynolds number is seen also a pair of counter-rotating secondary vortices symmetrically placed about the horizontal centreline near the centre of the right wall. Figures 4(c) and 4(d) show the streamline patterns for $Re = 1000$ and $Re = 2000$ respectively. It is seen that with the increase in Reynolds number the primary vortex cores move towards the centres of the top and bottom halves of the cavity and the secondary vortex pair grow in size. At all the Reynolds numbers the counter-rotating pairs of primary and secondary vortices maintain their symmetry about the horizontal centerline.

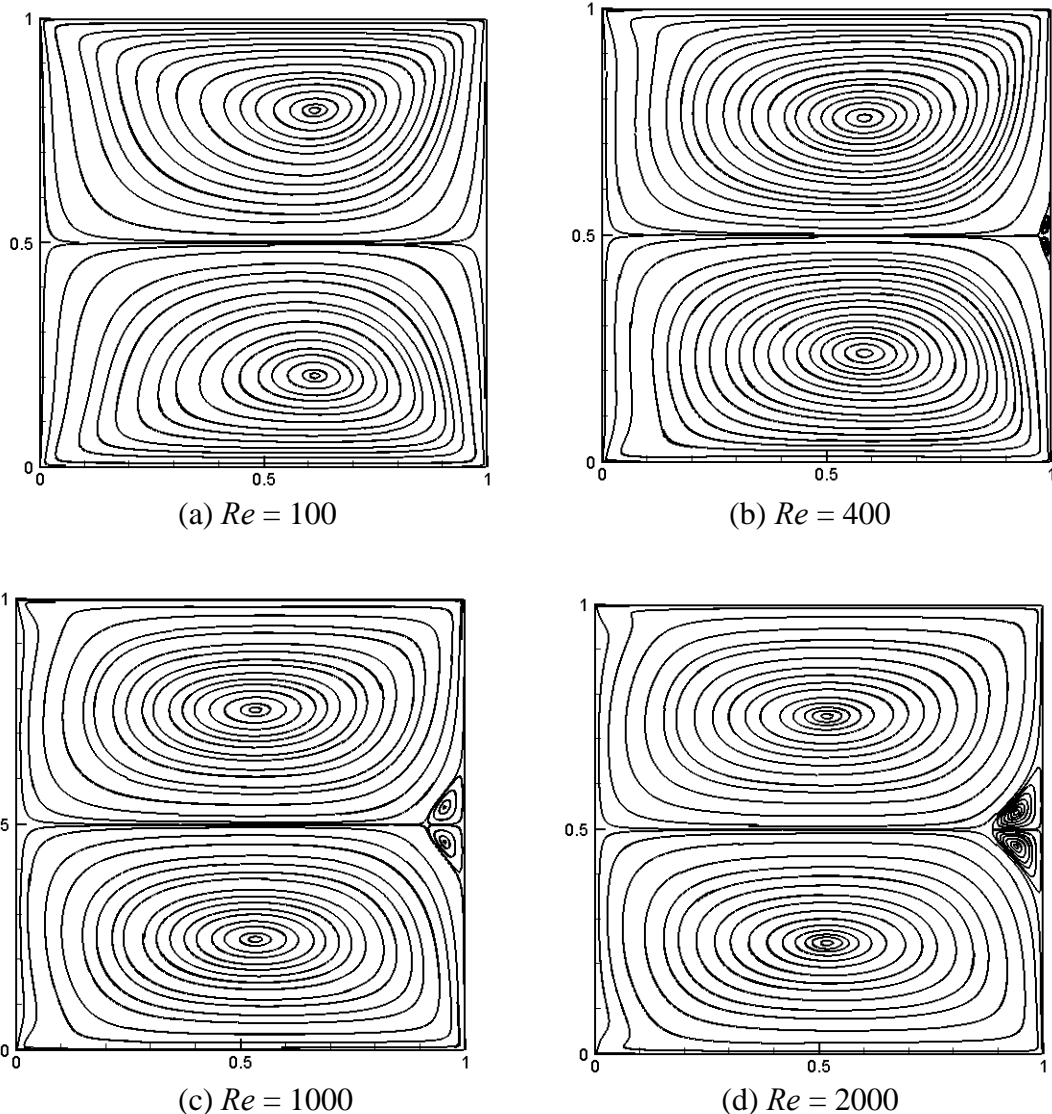


Figure 4. Streamline pattern for parallel wall motion at (a) $Re = 100$ (b) $Re = 400$
 (c) $Re = 1000$ and (d) $Re = 2000$ on a 513×513 lattice.

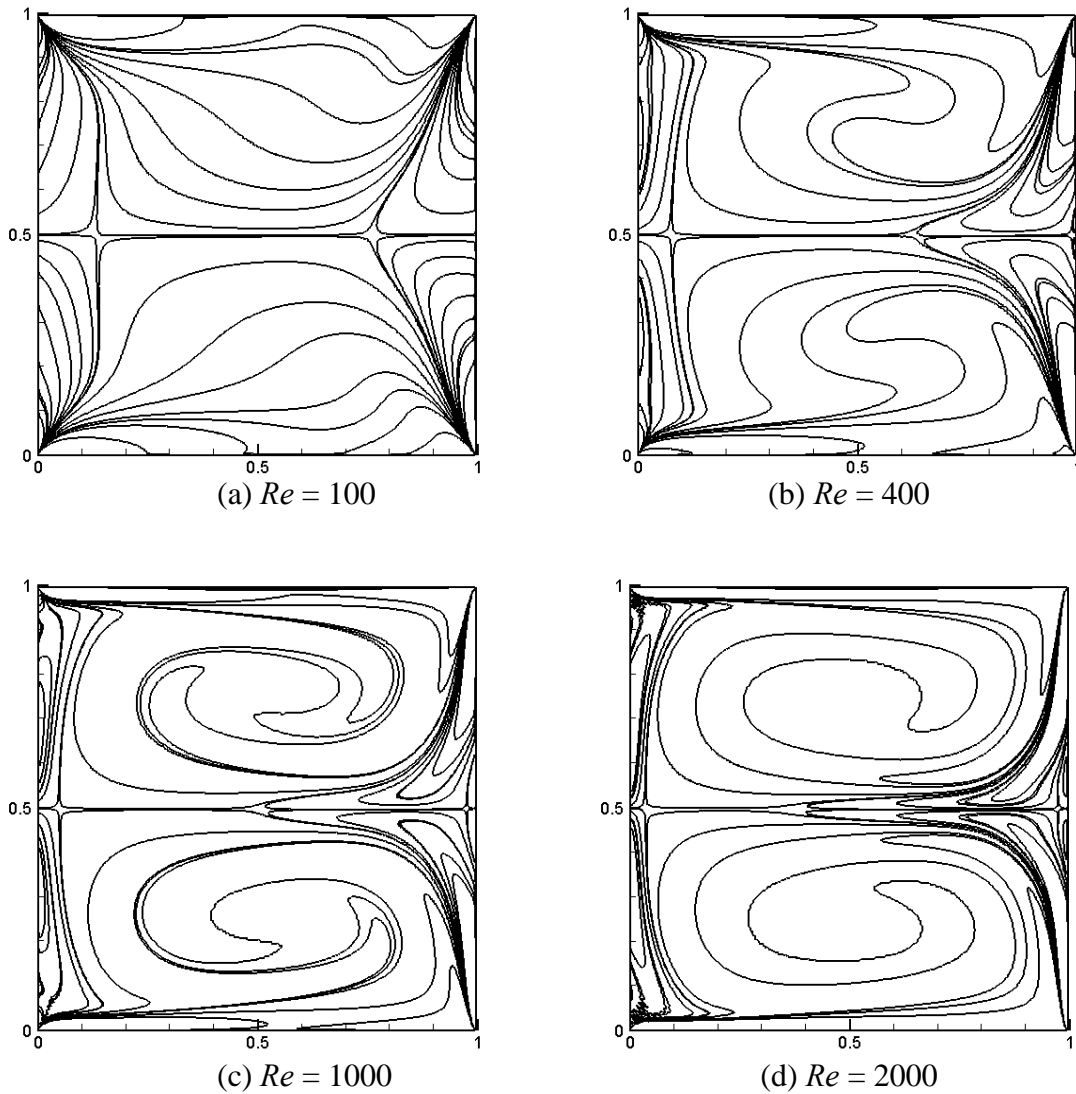


Figure 5. Vorticity contours for parallel wall motion at (a) $Re = 100$ (b) $Re = 400$
 (c) $Re = 1000$ and (d) $Re = 2000$ on a 513×513 lattice.

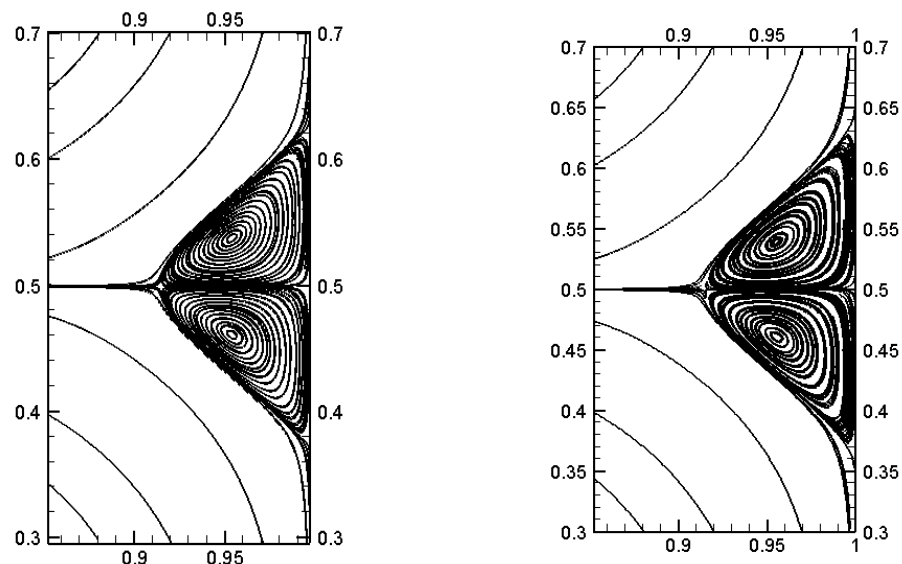


Figure 6. A magnified view of secondary vortices for parallel wall motion at $Re = 1000$
 (a) LBM, (b) FDM [1].

Figure 5 shows the vorticity contours. In Figure 6 a magnified view of the secondary vortices at $Re = 1000$ is compared with those obtained by FDM [1] to show that the vortices have been captured accurately. The other results are now authenticated by comparison with the same reference. Figures 7-10 show the comparison for horizontal velocity profiles along vertical lines and vertical velocity profiles along horizontal lines passing through different points of the cavity for various Reynolds numbers. Agreement of the velocity profiles given by LBM and FDM is once again excellent. Table 1 gives the locations of the vortices given by the LBM and FDM for $Re = 100, 400, 1000, 1500$ and 2000 . All these results show that the agreement is very good, which further substantiates the accuracy of the present LBM computations. We thus accurately list various flow details for this relatively unexplored configuration.

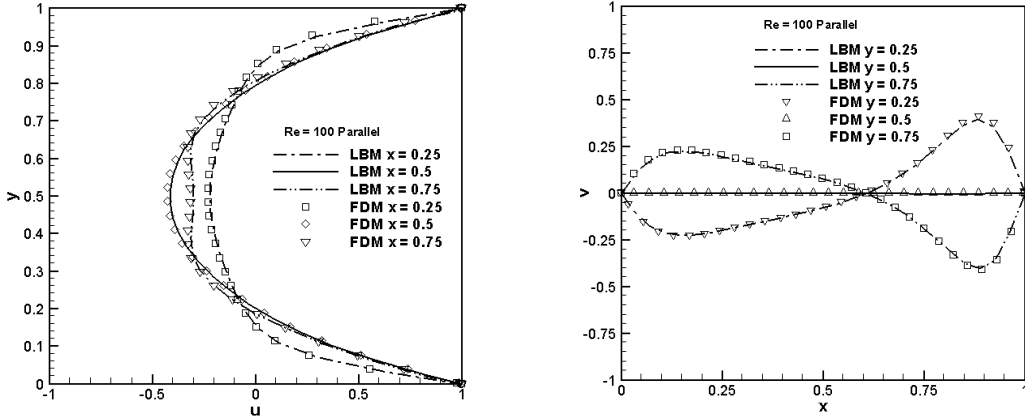


Figure 7. Parallel wall motion, $Re = 100$: (a) horizontal velocity u along vertical lines ($x=0.25, 0.50, 0.75$), (b) vertical velocity v along horizontal lines ($y=0.25, 0.50, 0.75$).

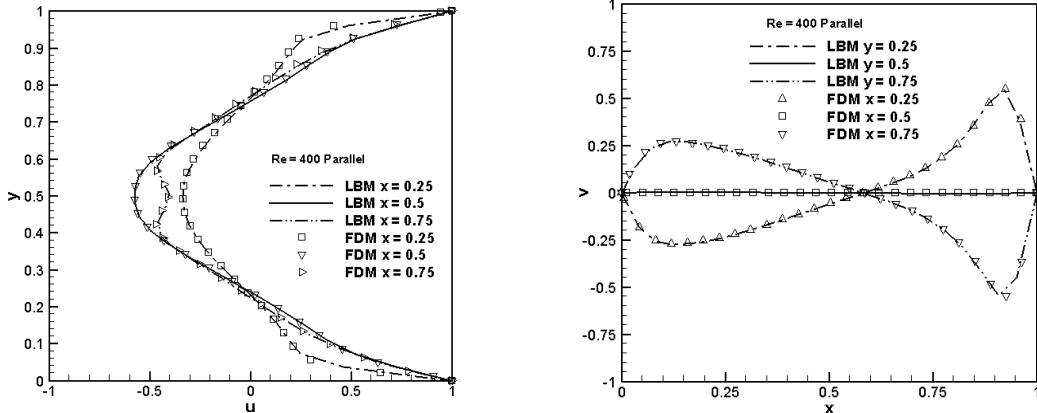


Figure 8. Parallel wall motion, $Re = 400$: (a) horizontal velocity u along vertical lines ($x=0.25, 0.50, 0.75$), (b) vertical velocity v along horizontal lines ($y=0.25, 0.50, 0.75$).

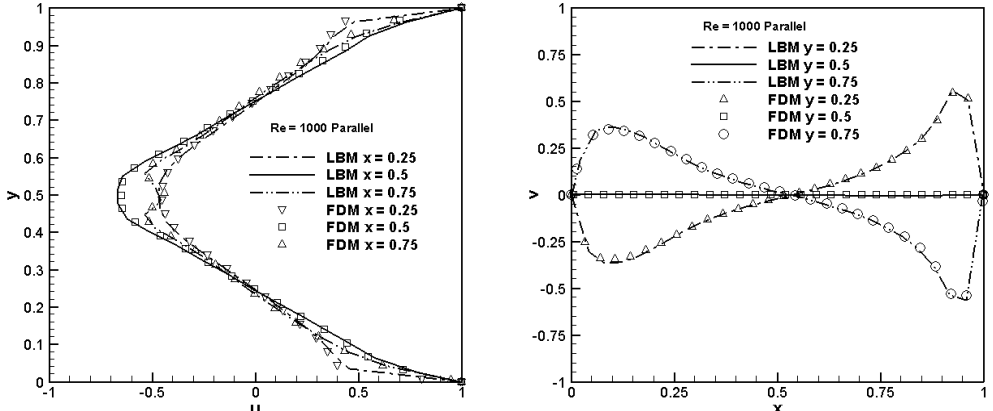


Figure 9. Parallel wall motion, $Re = 1000$: (a) horizontal velocity u along vertical lines ($x=0.25, 0.50, 0.75$), (b) vertical velocity v along horizontal lines ($y=0.25, 0.50, 0.75$).

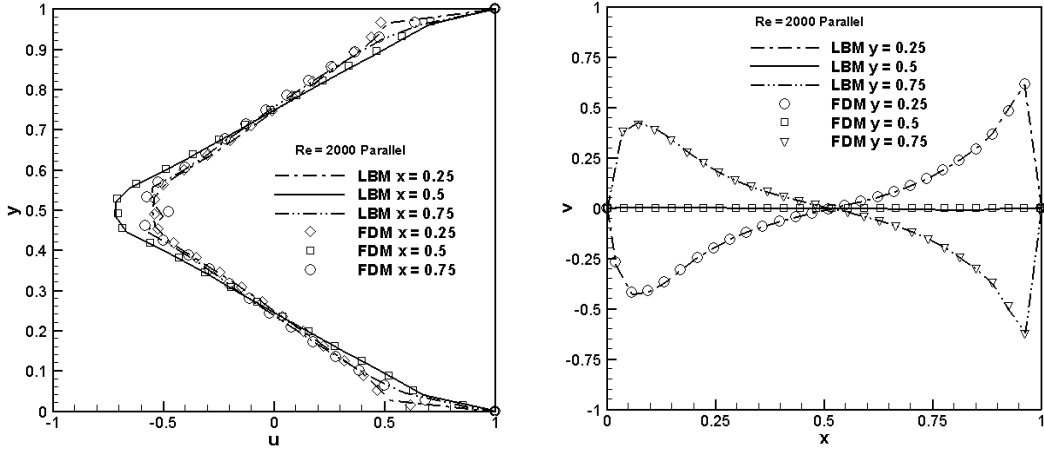


Figure 10. Parallel wall motion, $Re = 2000$: (a) horizontal velocity u along vertical lines ($x=0.25, 0.50, 0.75$), (b) vertical velocity v along horizontal lines ($y=0.25, 0.50, 0.75$).

TABLE 1: LOCATIONS OF THE VORTICES FOR PARALLEL WALL MOTION: a. FDM [1], b. LBM.

Re	Primary vortex centres				Secondary vortex centres			
	Bottom		Top		Bottom		Top	
	x	y	x	y	x	y	x	y
100	a. 0.6145	0.2026	0.6145	0.7959
	b. 0.6146	0.2027	0.6146	0.7957
400	a. 0.5845	0.2388	0.5845	0.7553	0.9873	0.4638	0.9873	0.5264
	b. 0.5846	0.2389	0.5846	0.7552	0.9874	0.4653	0.9874	0.5273
1000	a. 0.5354	0.2452	0.5354	0.7547	0.9551	0.4570	0.9551	0.5409
	b. 0.5342	0.2438	0.5342	0.7552	0.9542	0.4697	0.9542	0.5391
1500	a. 0.5246	0.2452	0.5251	0.7527	0.9443	0.4569	0.9444	0.5429
	b. 0.5239	0.2438	0.5239	0.7521	0.9439	0.4571	0.9439	0.5342
2000	a. 0.5132	0.2474	0.5132	0.7528	0.9400	0.4573	0.9400	0.5478
	b. 0.5108	0.2489	0.5108	0.7497	0.9378	0.4598	0.9377	0.5389

3.2. Antiparallel Wall Motion

In the antiparallel wall motion the upper and lower walls move in opposite directions along the x -axis with the same velocity. Figure 11 shows the streamline patterns on a lattice size of 513×513 for the antiparallel wall motion. A single primary vortex centred at the geometric centre of the cavity is formed at low Reynolds numbers as shown in Figure 11(a) for $Re = 100$ and Figure 11(b) for $Re = 400$. The streamline patterns for $Re = 1000$ and 2000 are shown in Figures 11(c) and 11(d) respectively. The increased Reynolds number results in the appearance of two secondary vortices near the top left and the bottom right corners of the cavity and a very small shift of the primary vortex centre from the geometric centre of the cavity. It will not be out of place to mention here that for the much-examined single lid-driven cavity flow the secondary vortex near the trailing edge of the moving wall does not appear at a Reynolds number as low as 1000 but much beyond that (at some value higher than 2000). It is also seen that with the increase in Reynolds number the shift of the primary vortex centre from the geometric centre of the cavity is small so that it remains very close to the geometric centre even

for these higher values of $Re = 1000$ and 2000 . However, in line with parallel wall motion, between $Re = 1000$ and 2000 the secondary vortices are seen to grow in size. The vorticity contours for various Reynolds numbers are shown in Figure 12. A magnified view of the secondary vortices (the ones at the top left corner) at $Re = 1000$ given by the present LBM and FDM [1] is shown in Figure 13. The agreement is found to be very good. Figures 14-17 show the comparisons for horizontal velocity profiles along vertical lines and vertical velocity profiles along horizontal lines passing through different points of the cavity for the various Reynolds numbers and the agreement is excellent once again. Table 2 gives the locations of the vortices given by the present LBM and FDM [1] for $Re = 100, 400, 1000, 1500$ and 2000 . Clearly the results given by the LBM agree very well with those of the FDM. We thus see that the LBM results given by all the figures and tables are in excellent agreement with those given by the FDM [1]. This lends credibility to the current LBM results for this problem.

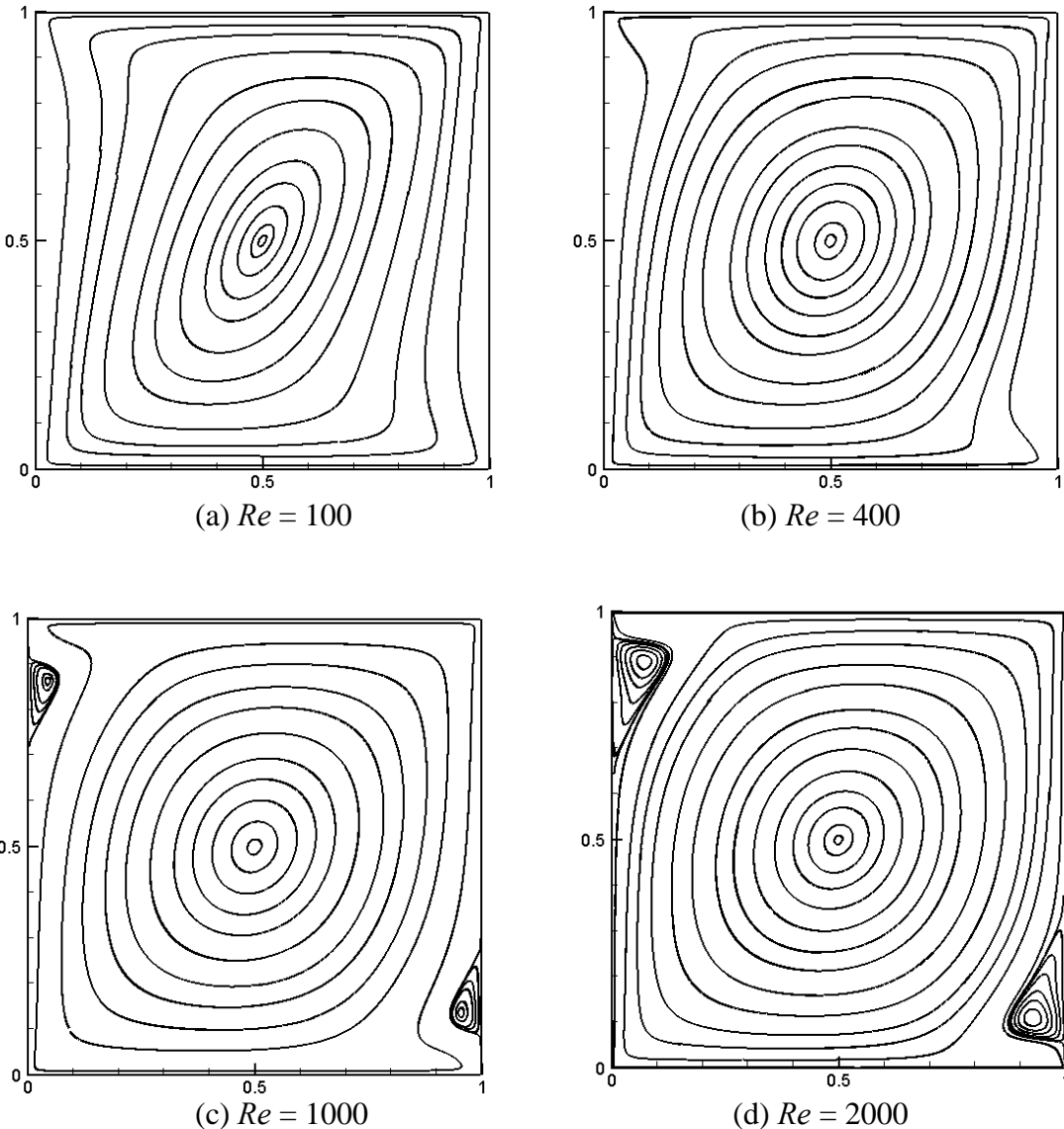


Figure 11. Streamline pattern for antiparallel wall motion at (a) $Re = 100$ (b) $Re = 400$ (c) $Re = 1000$ and (d) $Re = 2000$ on a 513×513 lattice.

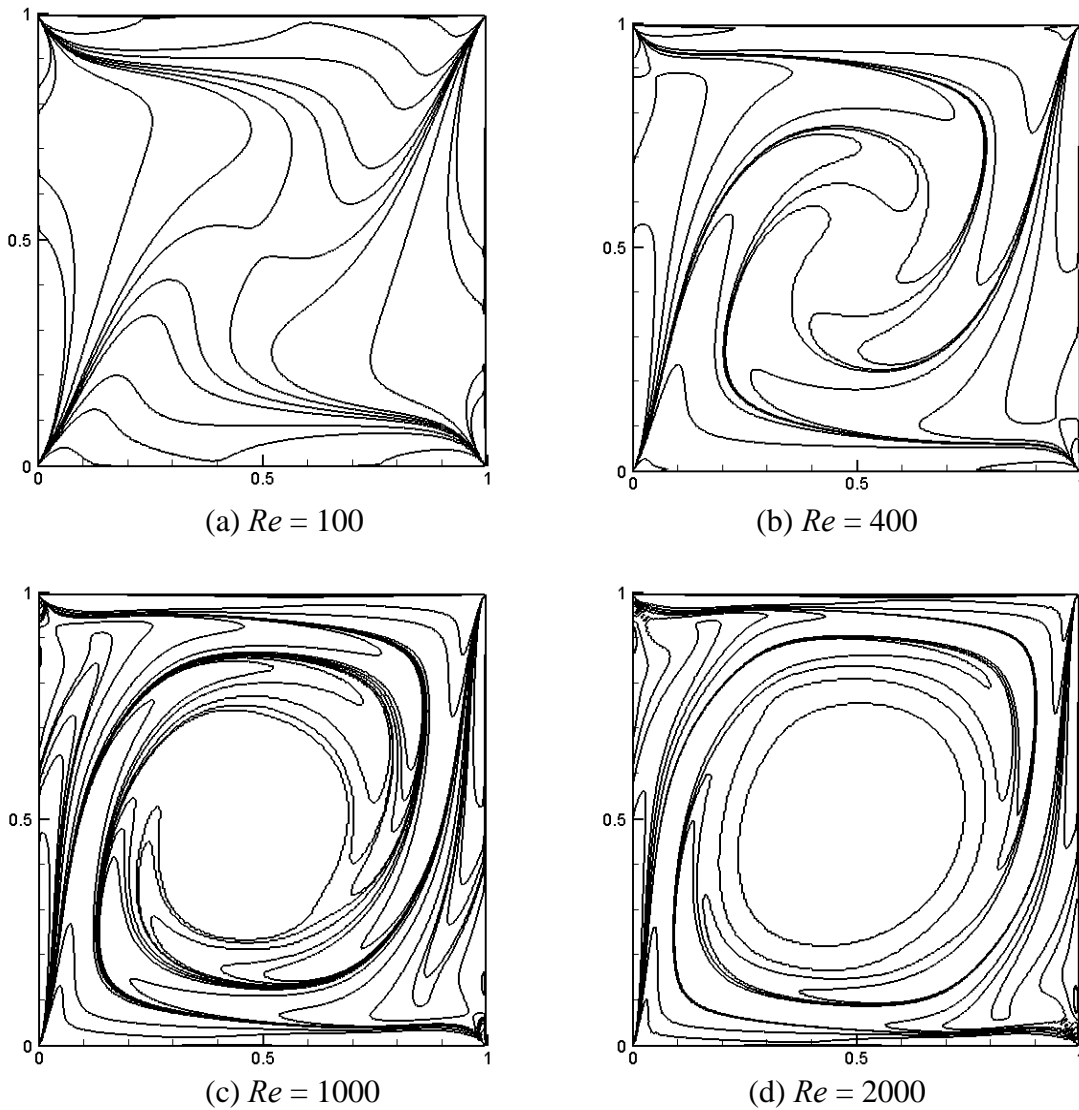


Figure 12. Vorticity contours for antiparallel wall motion at (a) $Re = 100$ (b) $Re = 400$
 (c) $Re = 1000$ and (d) $Re = 2000$ on a 513×513 lattice.

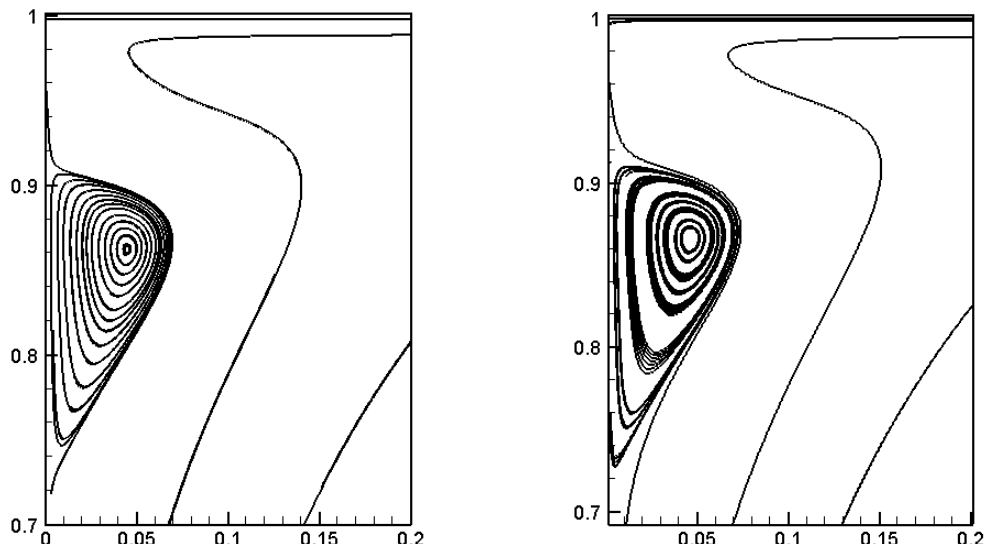


Figure 13. A magnified view of secondary vortices for antiparallel wall motion at $Re = 1000$
 (a) LBM, (b) FDM.

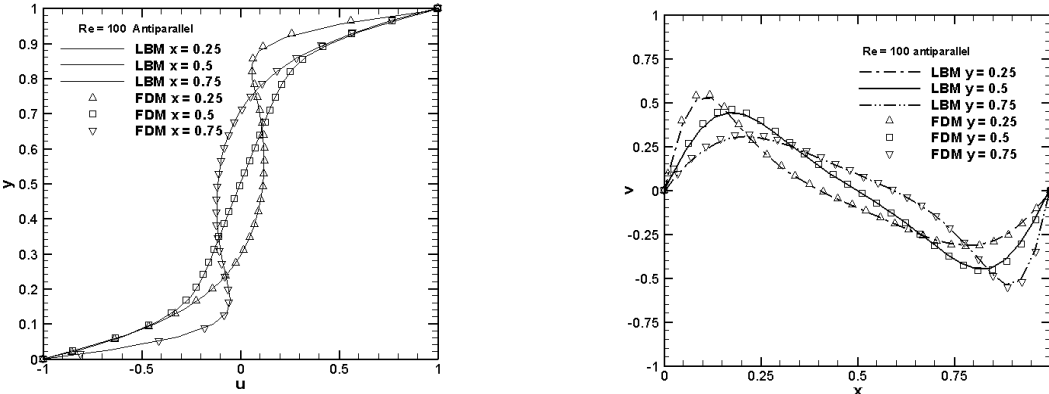


Figure 14. Antiparallel wall motion, $Re = 100$: (a) horizontal velocity u along vertical lines ($x=0.25, 0.50$ and 0.75), (b) vertical velocity v along horizontal lines ($y=0.25, 0.50$ and 0.75).

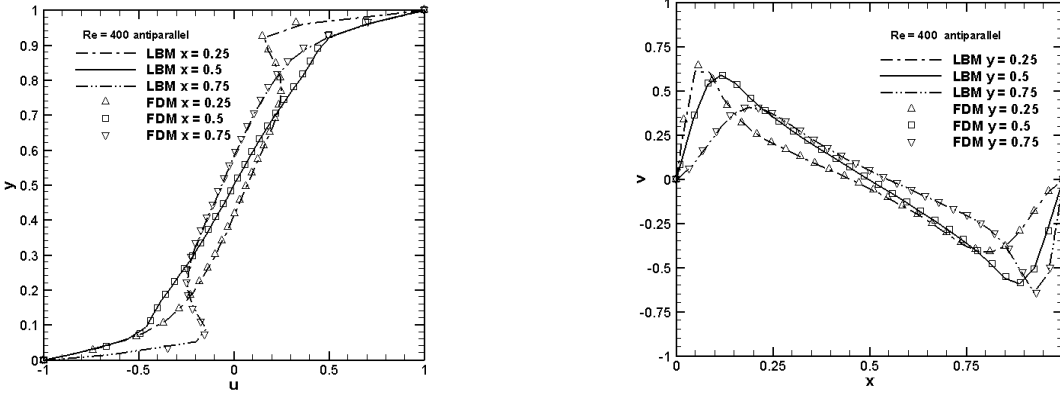


Figure 15. Antiparallel wall motion, $Re = 400$: (a) horizontal velocity u along vertical lines ($x=0.25, 0.50$ and 0.75), (b) vertical velocity v along horizontal lines ($y=0.25, 0.50$ and 0.75).

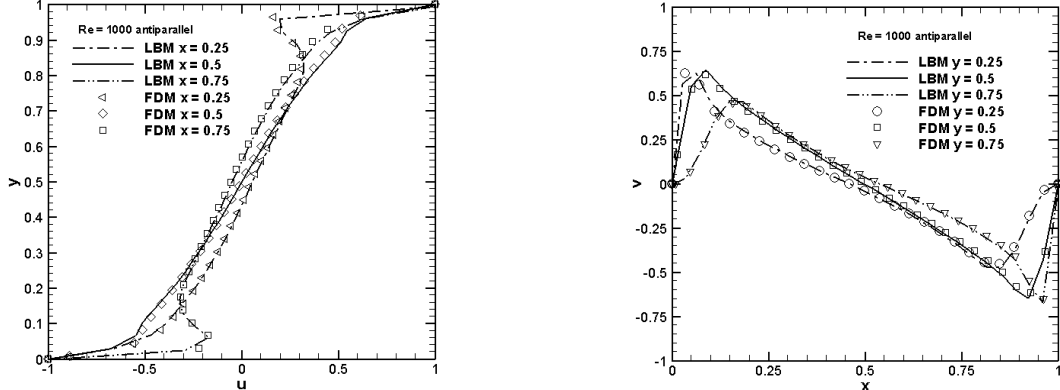


Figure 16. Antiparallel wall motion, $Re = 1000$: (a) horizontal velocity u along vertical lines ($x=0.25, 0.50$ and 0.75), (b) vertical velocity v along horizontal lines ($y=0.25, 0.50$ and 0.75).

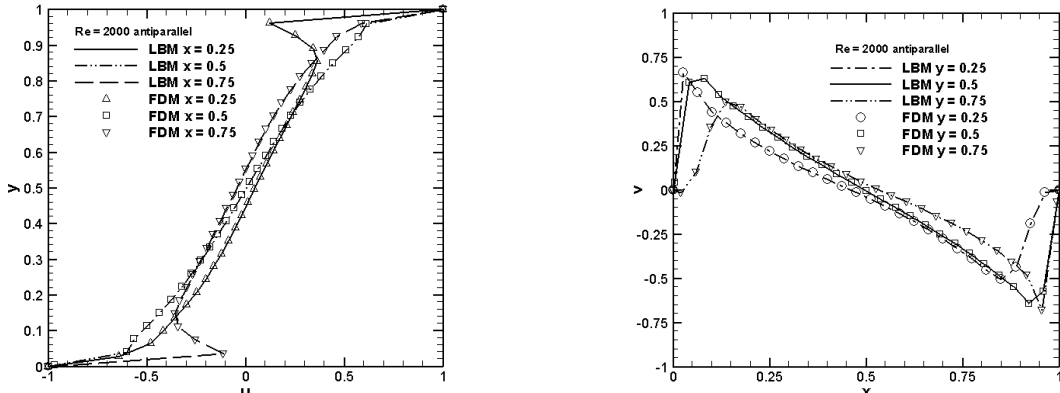


Figure 17. Antiparallel wall motion, $Re = 2000$: (a) horizontal velocity u along vertical lines ($x=0.25, 0.50$ and 0.75), (b) vertical velocity v along horizontal lines ($y=0.25, 0.50$ and 0.75).

TABLE 2: LOCATIONS OF THE VORTICES FOR ANTIPARALLEL WALL MOTION: (a) FDM [1], (b) LBM.

Re	Primary Vortex (PV)		Secondary Vortices (SV)			
	x	y	Bottom Right		Top Left	
			x	y	x	y
100	a. 0.5001	0.5002
	b. 0.5002	0.5001
400	a. 0.5002	0.4981
	b. 0.5001	0.4982
1000	a. 0.5009	0.4980	0.9507	0.1319	0.0492	0.8663
	b. 0.5011	0.4981	0.9499	0.1324	0.0478	0.8637
1500	a. 0.5007	0.4982	0.9308	0.1156	0.0692	0.8856
	b. 0.5009	0.4981	0.9317	0.1169	0.0681	0.8841
2000	a. 0.5002	0.5001	0.9227	0.1082	0.0771	0.8920
	b. 0.5003	0.4996	0.9238	0.1081	0.0761	0.8875

4. Conclusion

In this work a relatively unexplored flow configuration in a two-sided lid-driven square cavity is computed with the LBM. The flow is investigated for both the parallel and antiparallel motion of two of the facing walls. In the case of parallel wall motion, besides two primary vortices, there also appears a pair of counter-rotating secondary vortices symmetrically placed about the centerline parallel to the motion of the walls. About this centerline also appears a ‘free’ shear layer with the increase in Reynolds number. In the case of anti-parallel wall motion, besides a single primary vortex, there appears two secondary vortices near the trailing edges of the moving walls. Each of these near-tailing-edge vortices are seen to appear at a much lower Reynolds number compared with that in the single lid-driven cavity flow. The results of investigation of this relatively unexplored problem comprise figures and tables detailing streamlines and vorticity contours, various velocity profiles and features of vortices like their centres and shapes. All these LBM results compare very well with the only existing (and accurate) set of FDM results. This not only lends credibility to, but also benchmarks these results for the present flow configuration. Consequently these results, like those of the single lid-driven cavity flow, may be used for validating the algorithms for computing steady flows governed by the 2D incompressible Navier-Stokes equations.

References

- [1] Perumal, D.A, and A.K. Dass, *Simulation of Incompressible flows in two-sided lid-driven square cavities. Part I – FDM*, CFD Letters, 2(1), pp. 1-12.
- [2] Wolf-Gladrow, D.A., Lattice-Gas Cellular Automata and Lattice Boltzmann Models: An Introduction. 2000: Springer-Verlag Berlin-Heidelberg.
- [3] Succi, S., The Lattice Boltzmann Method for Fluid Dynamics and Beyond. 2000: Oxford University Press.
- [4] Chen, S., and G.D. Doolen, *Lattice Boltzmann method for fluid flows*. Annual Review of Fluid Mechanics, 1998. **30**: p. 282-300.
- [5] Hardy, J., Y. Pomeau, and O. de Pazzis, *Time Evolution of a Two-Dimensional classical lattice system*. Physical Review Letters, 1973. **31**: p. 276-279.
- [6] Frisch, U., B. Hasslacher, and Y. Pomeau, *Lattice-Gas automata for the Navier-Stokes equations*. Physical Review Letters, 1986. **56**: p. 1505-1508.
- [7] McNamara, G.R., and G. Zanetti, *Use of the Boltzmann Equation to Simulate Lattice-Gas Automata*. Physical Review Letters, 1988. **61**: p. 2332-2335.

- [8] Higuera., and Jimenez, *Boltzmann approach to Lattice Gas Simulations*. Europhysics Letters, 1989. **9**(7): p. 663-668.
- [9] Bhatnagar P.L., E.P. Gross and M. Krook, *A Model for Collision Processes in Gases. I. Small Amplitude Processes in Charged and Neutral One-Component Systems*. Physical Review, 1954. **94**: p. 511-525.
- [10] Koelman J.M.V.A., *A Simple Lattice Boltzmann Scheme for Navier-Stokes Fluid Flow*. Europhysics Letters, 1991. **15**(6): p. 603-607.
- [11] Chen S., H. Chen, Martinez and Matthaeus, *Lattice Boltzmann Model for Simulation of Magnetohydrodynamics*. Physical Review Letters, 1991. **67**(27): p. 3776-3780.
- [12] Qian Y.H., D. d'Humieres and P. Lallamand, *Lattice BGK Models for Navier-Stokes Equation*. Europhysics Letters, 1992. **17**(6): p. 479-484.
- [13] Chen H., S. Chen, and Matthaeus, *Recovery of the Navier-Stokes Equation using a lattice-gas Boltzmann method*. Physical Review A, 1992. **45**(8): p. R5339-5342.
- [14] Shankar, P.N, and M.D. Deshpande, *Fluid Mechanics in the Driven Cavity*. Annual Review of Fluid Mechanics, 2000. **32**: p. 93-136.
- [15] Kuhlmann H.C., M. Wanschura, and H.J. Rath, *Flow in two-sided lid-driven cavities: non-uniqueness, instability, and cellular structures*. Journal of Computational Physics, 1997. **36**: p. 267-299.
- [16] Ghia U., K.N. Ghia, and C.T. Shin, *High-Re solutions for incompressible flow using Navier-Stokes equations and a multigrid method*. Journal of Computational Physics, 1982. **43**: p. 387-411.
- [17] Hou, S., Q. Zou, S. Chen, G. Doolen, and A.C. Cogley, *Simulation of Cavity Flow by the Lattice Boltzmann Method*. Journal of Computational Physics, 1995. **118**: p. 329-347.
- [18] Perumal, D.A, and A.K. Dass, *Lattice Boltzmann Simulation of Two and Three Dimensional Flow in a Lid-Driven Cavity*. in *2008 Proceedings of the Int. Conference on Advances in Mechanical Engg, IC-ICAME-08*. 2008. IISc Bangalore, INDIA.
- [19] Lai Y.G., C.L. Lin, and J. Huang, *Accuracy and Efficiency study of a Lattice Boltzmann method for steady-state flow simulations*. Numerical Heat Transfer, Part B, 2001. **39**: p. 21-43.
- [20] Yu D., R. Mei, L.S. Luo, and W. Shyy, *Viscous flow computations with the method of lattice Boltzmann equation*. Progress in Aerospace Sciences, 2003. **39**: p. 329-367.